Construction and Building Materials 180 (2018) 23–34

Contents lists available at ScienceDirect

Construction and Building Materials

journal homepage: www.elsevier.com/locate/conbuildmat

Flexural performance of concrete beams containing engineered cementitious composites

Ali S. Shanour [a,*], Mohamed Said [a], Alaa Ibrahim Arafa [b], Amira Maher [a]

[a] Department of Civil Engineering, Shoubra Faculty of Engineering, Benha University, 108 Shoubra St., Shoubra, Cairo, Egypt
[b] National Housing and Building Research Centre (HBRC), Cairo, Egypt

HIGHLIGHTS

- Performance of concrete beams with Engineered Cementitious Composites ECC.
- Variable volume fractions of (PVA) and (PP) fibers were used.
- ECC materials exhibits an improvement in ductility.
- Load carrying capacity is more significant for using PVA rather than PP.
- Non-linear finite element analyses were performed and assessed with experimental results.

ARTICLE INFO

Article history:
Received 21 January 2018
Received in revised form 26 April 2018
Accepted 27 May 2018

Keywords:
Concrete beams
PVA fiber
Polypropylene fiber
ECC materials
Fiber reinforced concrete
Non-linear finite element analysis (NLFEA)

ABSTRACT

Engineered Cementitious Composites (ECC) considers a type of ultra-ductile cementitious composites with fiber reinforcement. It is developed for applications for economic purpose in the construction industry. ECC characterizes by strain hardening and multiple cracking. This paper experimentally investigates the performance of ECC concrete beams reinforced with conventional reinforcement bars. Advanced Polyvinyl Alcohol Engineered Cementitious Composite (PVA-ECC) fibers were selected in this purpose. Twelve RC beams were poured and tested to study flexure behavior under four-point loading test. Two different longitudinal reinforcement percentages, variable volume ratios of (PVA) and polypropylene fibers (PP) were used. optimizing the usage of PVA material trails to put it in the lower layer of the section at point of maximum tension with variable thicknesses was conducted. Initial flexure cracking load, ultimate load, the ductility and the load-to-deflection relationship at various stages of loading were evaluated. Experimental outcomes revealed that the enhancement in maximum capacity is more significant in the case of using PVA rather than PP. The maximum load increases by 20% and 34% for 1.0% and 2.0% of PVA contents in total section respectively. The relative ductility factor increases by 30% and 45% for 1.0% and 2.0% of PVA content. Results also depicted that a reasonable considerable increasing in the load capacity when used limited layer thickness of PVA concrete. Nonlinear Finite Element Analysis (NLFEA) was conducted for the purpose of simulating the behavior of experimentally tested beams, regarding crack behavior and load-deflection response. Reasonable agreement was achieved between the experimental results and NLFEA results.

1. Introduction

The development of fiber reinforcing material for concrete has undergone at the few last decades. In the 1960's, the effectiveness of short steel fibers in reducing the brittleness of concrete was studied [12,11]. This improvement has continued using extension of varied fiber types, such as carbon, glass, and synthetics. Recently, hybrids mixture in which a combination of varied fiber types or fiber lengths has been arises. Concrete with discrete fibers, like polypropylene exhibits drop in the tensile resistance as a distinct crack expands during tension-softening, (PVA-ECC) fiber is considered a promising alternative for fiber reinforced concrete [15]. Deformation for ECC during the elastic and strain-hardening phases is suitably defined as straining. The tensile resistance continues to rise during multiple micro cracking and the strain increased continuously. Based on the load-to-deflection curve of

* Corresponding author.
E-mail addresses: ali.shnor@feng.bu.edu.eg (A.S. Shanour), mohamed.abdelghaffar@feng.bu.edu.eg (M. Said).

https://doi.org/10.1016/j.conbuildmat.2018.05.238
0950-0618/

concrete, the participation of concrete in uni-axial tension can be defined as the tension-stiffening effect [1].

ECC concrete reveals its tensile ductility under tension load [7,16,17,6,8]. When ECC concrete beam subjected to bending, a multiple micro-cracking mechanism was formed at the zone of maximum tension stresses. In addition, allowing it to encounter a high curvature progress – an occurrence that has resulted in the general name of "bendable concrete". Regardless the element geometry, deflection hardening is an essential property of ECC. This is not the response for tension-softening FRC beam, in which deflection hardening comes to be challenging to achieve as beam depth increases [13]. The cost of PVA is estimated about 1/8 of high modulus polyethylene (PE) fiber, and is even less than steel fiber of the same volume basis. With some certain improvements in fiber properties, PVA fiber introduces a promise as ECC reinforcement [15].

Yuan et al. [18], studied the effects of the ECC concrete layer thickness and position on the manners of the steel reinforced specimens with ECC/concrete composite. The stresses provided by ECC at tension region lead to larger area of concrete participating in compression. Hence, the maximum moment capacity was enhanced. Doo-Yeol Yoo et al. [4], investigated the behavior of beams including ultra-high performance ECC. They recorded a strain-hardening characteristic though the formation of fine micro cracks at failure load. PAN JinLong et al. [10], carried out a four-point load test to study the flexural characteristics of PVA with different ratio. It concluded that the ductility and bending strength of ECC material are significantly larger than those of plain concrete. In addition, when the volume fraction increased, the ductility increases.

Alfonso [2], was presented the results of flexural behavior eight beams with SFRC external layers and RC internal layer. The SFRC beams exhibited 70% greater energy absorption than RC beam. Fang et al. [5], tested beam-column joints with ECC composite exposed to cyclic loads. According to the results, the additions of ECC materials in joint zone significantly enhance the load capacity and ductility. In addition, the higher shear strength and ductility of ECC concrete, the higher the energy dissipation encountered. D. Nicolaides et al. [3], established a constitutive material model by using the extracted results from the experimental outcomes of beams with fiber reinforcement and subjected to three-point bending tests. Inverse analysis (least-square method) method was used to develop a material model for which reaching to optimum correlation between the test results and numerical load-deflection relationships. Most of the previous research works were limited to use one kind of fiber as ECC material. for that reason, the performance of beams with ECC material using mix of two kinds of fiber need to be investigated.

The aims of this paper are, experimentally and analytically investigate the performance of beams with ECC regarding the cracking load, ultimate load, the ductility and the load-to-deflection response. Two kinds of fibers were used for that purpose, ECC in the form of PVA and polypropylene PP fiber. The paper aims also to develops a numerical models using (NLFEA) to simulates ECC beams performance and help to conducts more future parametric studies. The developed numerical models were performed using ANSYS software [22].

2. Test program

2.1. Test specimens

In this investigation, twelve concrete beams were cast. Two control beams were poured without fibers for comparison, and the rest of specimens included fibers. Two types of fiber materials have been utilized in this investigation; ECC material in the form of Poly viny1alchol fibers (PVA) and Polypropylene fibers (PP). The geometrical and mechanical properties of the used fibers were measured, Sayed et al. [23]. PVA fibers have a length of 12 mm, a diameter of 39 μm, an elastic modulus of 42.8 GPa, nominal strength of 1620 MPa and 6.0% elongation. Polypropylene fibers (PP) have a length of 12 mm, a diameter of 22 μm, an elastic modulus of 3.45 GPa, nominal strength of 550 MPa and 21.0% elongation. Two specimens were poured without adding any fiber as control beams with longitudinal reinforcement two 16 mm diameter and two 12 mm diameter respectively. Another two beams were cast totally with PVA volume ratio of 1.0% and 2.0%. Two more beams were cast totally with PVA and PP fibers with volume ratio of 0.50% and1.0% for each fiber. Three more beams containing 200 mm layer of PVA and PP fibers with volume content of 0.50% and 1.0% were casted. Three more beams containing 100 mm layer of PVA and PP fibers with volume content of 0.50% and 1.0% were cast. The cross sectional dimensions and the span of the specimens were kept constant for all the ten beams. The dimensions of all specimens were 115 mm x 280 mm x 1850 mm. Seven beams were reinforced using two steel bars of 16 mm diameter at the bottom face that serves as the main reinforcement, the other five beams were reinforced using two of 12 mm diameter. The yield stress was measured to be 400 MPa. Two bars of 8 mm diameter were used as top RFT and 8 mm diameter stirrups @ 100 mm c/c spacing were used as shear reinforcement as presented in Fig. 1 and Table 1.

2.2. Test setup

The specimens were tested in a machine of 1000 kN capacity. Beams were simply supported over a span of 1650 mm. The load was distributed on two plates kept 350 mm apart. The two loads are symmetrical to centerline of the beam. The dimension between the two loading plates is 350 mm. the edge dimension between the load plate and the nearest support is 650 mm. The specimens were tested under load control with the rate of 30–70 increments to failure. Strain gauges have been fixed at the longitudinal reinforcement bars to record the strain in the steel bars as illustrated in Figs. 2 and 3. Deflection at the centerline was measured for every 0.5 kN increment of load using a linear variable differential transformers (LVDT) fitted at the center. The cracks during loading stages were mapped out and other observations were recorded during loading and at the failure; Fig. 4 shows crack propagation of beam B1.

3. Experimental results and discussion

3.1. Initial crack load and ultimate load

All beam specimens were visually observed till the initial crack occurred, the corresponding load was noted. Table 2 provides a summary of the important experimental results for tested specimens. The load at initial crack increases as the volume content of fibers increases. PVA and PP material improve the residual strength of concrete through additional fracture energy. After the first cracks, fibers began to work during applying loads up to failure. However, with the addition of polypropylene fibers (PP), the increase in ultimate load is very marginal compared to (PVA). Compared to control beam B1 for group A, the maximum load increases by 20% and 34% for 1.0% and 2.0% of PVA fibers content ratio in total section, respectively. The increasing ratio reaches to 11% and 24% when using a mixer of both PVA and PP fiber with the ratios of 0.5% and 1.0% for B4 and B5, respectively. It can be noticed that using both PVA and PP with the volumetric ratios, 0.5% and

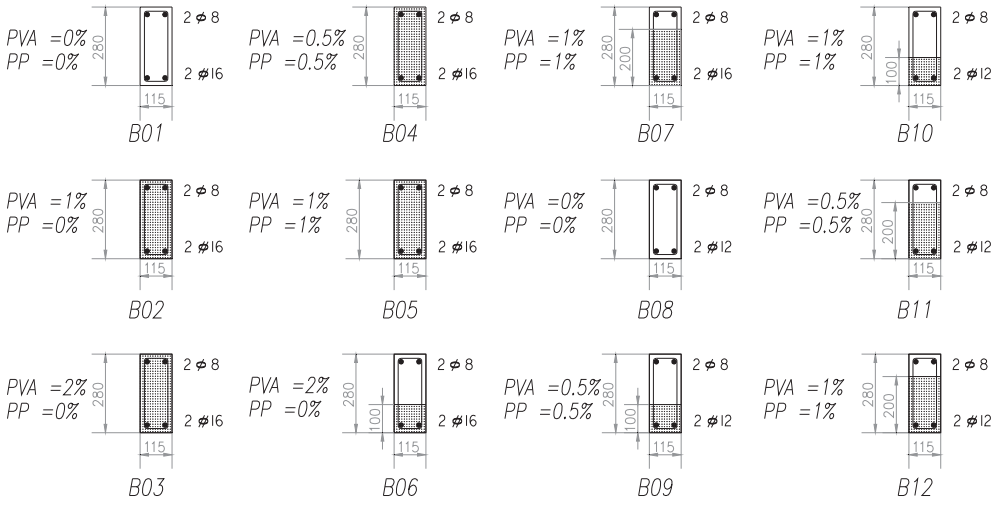

Fig. 1. Tested beams geometry and details.

Table 1
Detail of test beams.

Groups	Specimen	Concrete cube compressive strength (MPa)	Fiber content (PVA)V_f %	Fiber content (PP)V_f %	Thickness of Layer (mm)	Bottom RFT.		Transverse RFT.	
						Bars	Yield strength (MPa)	Bar size (mm)	Yield strength (MPa)
Group A	B1	55	0.00	0.00	———	2Ø16	400	10Ø8/m'	240
	B2	55	1.00	0.00	280	2Ø16	400	10Ø8/m'	240
	B3	55	2.00	0.00	280	2Ø16	400	10Ø8/m'	240
	B4	55	0.50	0.50	280	2Ø16	400	10Ø8/m'	240
	B5	55	1.00	1.00	280	2Ø16	400	10Ø8/m'	240
	B6	55	2.00	0.00	100	2Ø16	400	10Ø8/m'	240
	B7	55	1.00	1.00	200	2Ø16	400	10Ø8/m'	240
Group B	B8	55	0.00	0.00	———	2Ø12	400	10Ø8/m'	240
	B9	55	0.50	0.50	100	2Ø12	400	10Ø8/m'	240
	B10	55	1.00	1.00	100	2Ø12	400	10Ø8/m'	240
	B11	55	0.50	0.50	200	2Ø12	400	10Ø8/m'	240
	B12	55	1.00	1.00	200	2Ø12	400	10Ø8/m'	240

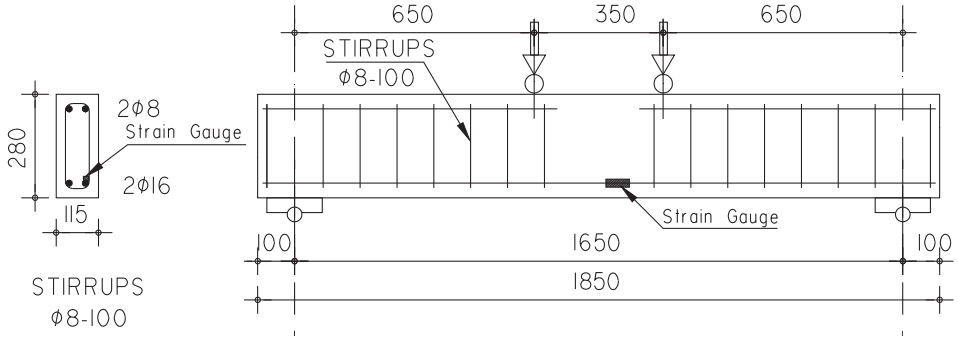

Fig. 2. Testing setup details.

1.0%, give lower gain in the load capacity when compared with the same ratio of only PVA fibers. Therefore, ECC fibers exhibits much better behavior than discrete fibers. The increase in load carrying capacities when using ECC material might be due to strain hardening and multiple micro-cracking behavior of ECC. An attempt to optimize usage of PVA material is to put it in the lower layer of the concrete section at a point of maximum tension. This is conducted through 100 mm and 200 mm thick layer of concrete containing PP and/or PVA fibers as depicted earlier in Fig. 1 for B6 and B7, respectively. The results reveal that a reasonable increasing in the load capacity in which it reaches 25% and 20% for B6 and B7, respectively.

Yuan et al. [18], found that increasing ECC layer enhance the moment capacity. They reached that the moment capacity increases linearly with the increase in ECC thickness. With increasing the ECC thickness, the tension region is strengthened and the

Fig. 3. Typical beam during testing.

Fig. 4. Crack propagation of beam B1.

neutral axis shifts downwards. The stresses provided by ECC in the tension zone lead to larger area of concrete participating in compression. The maximum moment capacity is hence improved.

For Group B, which has longitudinal reinforcements less than Group A, the load increases, in a 100 mm layer of the beam cross section, by 10% and 25% for 0.5% and 1.0% by mixing both of PVA and PP fiber content ratio respectively. On the other hand, the percentage of increasing reaches to 19% and 39% when using a mix of both PVA and PP fiber with the ratios of 0.5% and 1.0% for B11 and B12, respectively. Suji et al. [21], were recorded 18.6% to 34.39% increase in the ultimate load carrying capacity of the beams containing fibers.

3.2. Ductility factor (DF)

ECC materials exhibit an improvement in ductility. It reaches the extreme strength in the post- cracking deformation regime in addition to a relatively large inelastic deformation capability. Dancygier et al. [20] obtained higher structural ductility in beam specimens with fibers. An attempt was made in this study to obtain the (DF) for tested beams. The ductility factor can be defined as the percentage of the deflection at maximum load (δ_u) to the deflection when steel RFT starts to yield (δ_y). The values of (DF) are depicted in Table 3. Concrete beams with PVA material have more ductile behavior than the control beam. It was noted that in the case of PVA, as the fiber volume ratio increases, the ductility also increases. Comparing the relative ductility factor to control beam B1 for Group A, the relative ductility factor increases by 30% and 45% for 1.0% and 2.0% of PVA volume ratio in the beams' cross section. However, when using a mix of both PVA and PP fiber with the ratios of 1.0%, (DF) increased by 36% which indicate slightly higher than B1 due to adding PP fiber. For Group B, the ductility of specimens in this group exhibits low ductility than Group A due to lower longitudinal reinforcements. The (DF) increases by 32% and 13% for 0.5% and 1.0% mix of both PVA and PP fiber content ratio, in 100 mm layer of the cross section. On the other hand, the ductility improvement reaches to 16% and 90% when using a mix of both PVA and PP fiber with the ratios of 0.5% and 1.0% for B11 and B12, respectively.

3.3. Load-deflection response

The experimental load to mid-span deflection curves are depicted in Figs. 5 and 6. The plots represent the deflection value measured by the LVDT mounted at mid-span of beam. In general, the load-deflection curve consists of three main regions, the first region is a linear zone that specifies the response till the initial cracks, the second region is also a linear zone that represents the response till the yield of longitudinal reinforcement and the third region indicates the response after the yielding of reinforcement. At this region, high rate of increasing deflection took place for successive loads. It can be obviously found that specimens containing PVA and PP exhibit higher mid-span deflection before failure with extended ductile plateau more than control beam specimen as shown in Fig. 5a and b. Beam specimens with a 100 mm and 200 mm thickness of both PVA and PP exhibit rational ductility, and an increase in the load capacity. Fig. 6, shows that the specimen

Table 2
Experimental results.

Groups	Beam specimen	Fiber content (PVA)V_f %	Fiber content (PP)V_f %	Thickness of Layer (mm)	Initial racking load, P_{CT} (kN)	Ultimate load, P_{EXP} (kN)	Strength gain factor	Maximum Mid-span Deflection (mm)
Group A	B1	0.00	0.00	———	29.0	115	1	31
	B2	1.00	0.00	280	33.0	138	1.2	46
	B3	2.00	0.00	280	34.0	154	1.34	48
	B4	0.50	0.50	280	30.0	127	1.11	23
	B5	1.00	1.00	280	28.0	143	1.24	46
	B6	2.00	0.00	100	31.0	144	1.25	40
	B7	1.00	1.00	200	32.0	139	1.2	37
Group B	B8	0.00	0.00	———	26.0	81	1	19
	B9	0.50	0.50	100	30.0	89	1.1	25
	B10	1.00	1.00	100	29.0	101	1.25	22
	B11	0.50	0.50	200	28.0	96	1.19	23
	B12	1.00	1.00	200	30.0	109	1.35	38

Table 3
Ductility factor.

Groups	Beam specimen	Fiber content (PVA) V_f %	Fiber content (PP) V_f %	Thickness of Layer (mm)	Deflection at ultimate load (δ_u)	Deflection at yield load (δ_y)	Ductility Factor (δ_u/δ_y)	
							Absolute	Relative
Group A	B1	0.00	0.00	–––	31	5.6	5.5	1
	B2	1.00	0.00	280	46	6.5	7.1	1.3
	B3	2.00	0.00	280	48	6.0	8.0	1.45
	B4	0.50	0.50	280	24	5.3	4.5	0.82
	B5	1.00	1.00	280	46	6.1	7.5	1.36
	B6	2.00	0.00	100	40	7	5.7	1.04
	B7	1.00	1.00	200	37	7.2	5.1	0.93
Group B	B8	0.00	0.00	–––	19	5.1	3.7	1
	B9	0.50	0.50	100	25	5.1	4.9	1.32
	B10	1.00	1.00	100	22	5.3	4.2	1.13
	B11	0.50	0.50	200	23	5.3	4.3	1.16
	B12	1.00	1.00	200	38	5.4	7.0	1.9

B12 has the maximum ductility compared to the beams in Group B high ductility. It may be attributed to the high fiber volumetric ratio for low reinforcement ratio. For all specimens, it was not possible to forecast the concrete cracking load exactly from the load-deflection curve. Therefore, the first crack load was noticed only through the visual observation made during testing.

3.4. Mode of failure

Specimens were experimentally tested for flexure by applying four-point loading tests. The failure type was recorded as a flexure failure for all beams. The beams showed initial cracking in the high bending moment region and then the cracks propagated in the vertical direction as the load was increased. At approximately 80–90% of the ultimate load, shear cracks appeared near the supports and proceeded towards the compression zone. As mentioned previously, ECC material demonstrates strain hardening property, therefore, it could sustain tension load after cracking and it could be indicated that the load capacity would have increased. At the stage of ultimate failure, crush in compression region of concrete was observed in all specimens. Beams for Group A showed the same pattern of failure and the modes of failure are shown in Fig. 7a to g. Xu et al. [14], recorded similar mode of failure for concrete beams strengthened with ECC layer.

Fig. 8a to e show the crack pattern and failure mode for Group B. It can be seen that the same failure mode as illustrated for Group A was exhibited.

4. Non-linear finite elements analysis (NLFEA)

(NLFEA) was conducted to modeling the tested beams. Software package, ANSYS (ANSYS release 9.0) [22], was the current procedure to conduct the analytical study. The load-deflection curve is the important aspect in verifying the specimen's behavior. It includes response parameters such as ultimate loads, first cracking load, and maximum deflection. Therefore, comparing the load-deflection curves extracted from analytical results with experimental curves is considered an efficient method to validate the non-linear model.

Beams were modeled using 1998 equal-size isoparametric 3-D; Solid65 elements as presented in Fig. 9a. Solid65 element haves the capability of plastic deformation, three directions cracking, and crushing. The concrete material model is characterized by its capability to predict the failure of brittle materials. Both cracking and crushing failure modes are accounted for. The failure surface is shown as 3-D failure surface in principal stress space [22]. Flexural and shear reinforcements were modeled as discrete reinforcement using 3D spar elements (Link 8) as shown in Fig. 8b. This element includes two nodes and three DoF. Link 8 also haves the capability of plastic deformation. Bilinear kinematic hardening model was used for steel reinforcement. The fiber reinforcements were modeled as smeared reinforcements in the Solid 65 element represented through volumetric ratio to represent the actual fiber volumes used in each beam specimen. Mohamed et al. [9], used the same elements and procedures for modeling concrete beams with GFRP bars. They get reasonable agreement comparing test results.

4.1. NLFEA model verification

NLFEA results were compared to the experimental results of all beams. Flexural first cracks started when the cracking moment reached in the pure bending zone. Cracks were first observed at the zone of maximum tension near the high moment zone at mid-span. The cracks start to propagate in an upward direction through the beam depth. New cracks take place near the shear region by increasing the load, as presented in Fig. 10.

Referred to Table 3, NLFEA showed a first formation of vertical cracks in the mid-span at loads of 24–36 kN. The predicted cracking loads; $P_{c\text{-}nu}$ were revealed to be in a reasonable convention with the experimental loads; $P_{c\text{-}exp}$ with a mean $P_{c\text{-}nu}/P_{c\text{-}exp}$ ratio of 1.06 and a coefficient of variation (C.O.V) of 7.3%. Comparison between the numerical and experimental ultimate loads are listed in Table 4. It can be observed from Table 4 that, reasonable agreement was achieved between the test results and the analytical results. The percentage of the predicted to experimental ultimate strength for the beams ranged between 0.94 and 1.10, with a mean value of 1.05 and a coefficient of variation, C.O.V, of 5.4%. Implicitly, the analysis reflected the significance of test parameters investigated on the load-carrying capacity.

4.2. Load- deflection comparison

The load-deflection responses recorded by the numerical model were compared to the experimental results where good convention has been achieved. Comparison of the load-deflection plots obtained from ANSYS and experiments for all the ten beams are presented in Figs. 11 and 12 for Group A and Group B, respectively. Thus the numerical model developed using ANSYS has shown to provide accurate prediction of the load–deflection behavior of PVA & PP fiber reinforced beams. Slight deviations in the load-deflection curves could be illustrated as follows:

1. In the experimentally tested beams, micro cracks produced by drying shrinkage in the concrete were observed whereas the numerical model does not include the effect of micro cracks.

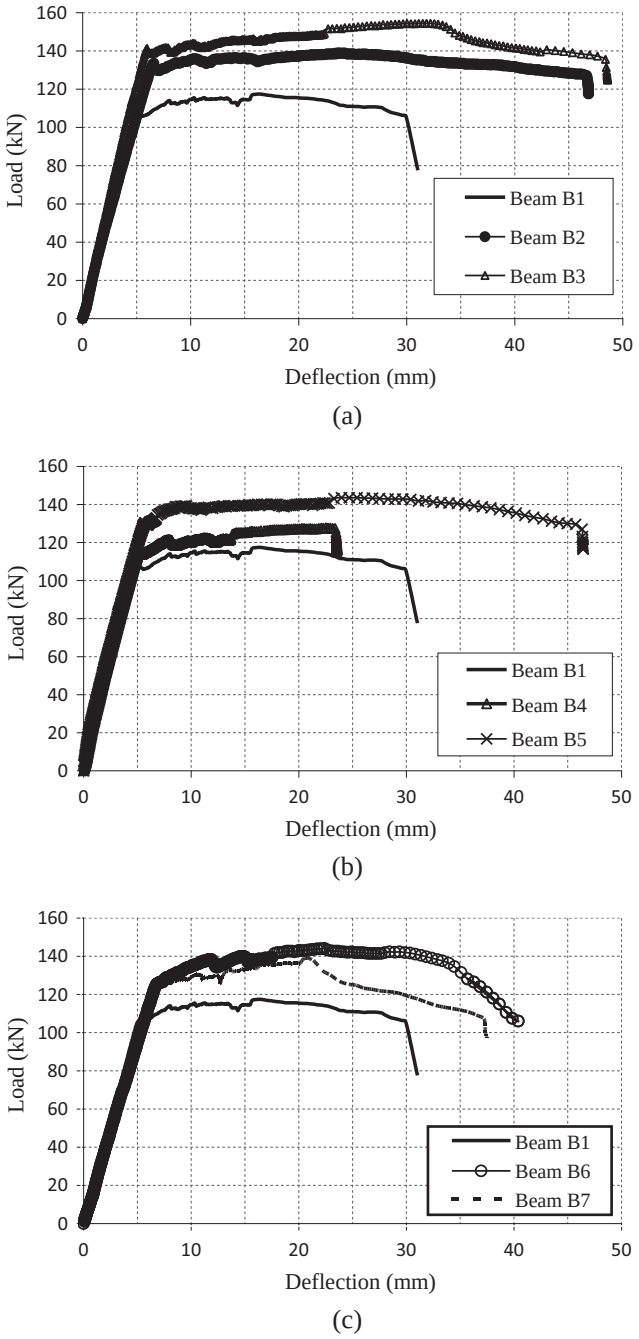

Fig.5. Load–midspan deflection of tested beams for Group A.

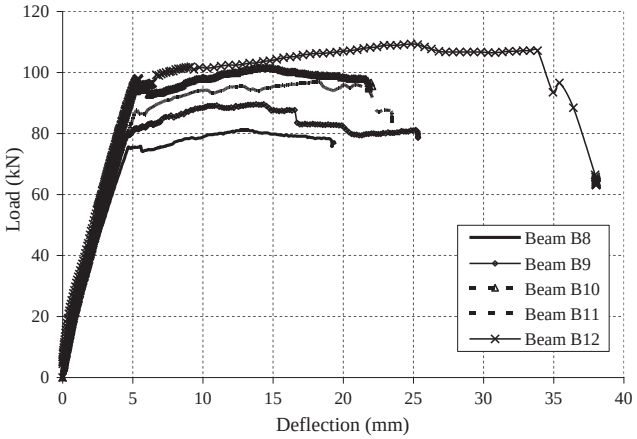

Fig.6. Load–midspan deflection of tested beams for Group B.

2. In the finite element analysis, perfect bonding is assumed between the concrete and the steel reinforcement, but the same assumption would not be true for the experimentally tested beam. The current model reasonably predicted the behavior of the specimens after cracking and up to 98% of failure load. In conclusion, to the range of the test parameters investigated, the application of NLFEA model presented in current study yielded satisfactory cracking load, load-carrying capacity, and load-deflection relationship.

5. Ultimate moment strength

The experimental ultimate moment capacity M_{exp} for each beam was calculated (using the relation $P/2$*0.65, where P is the failure load). In the purpose of comparing experimental results with design code equations, ACI code was introduced.

ACI Committee 544 [19] represents equation to estimate the nominal moment M_n of a singly reinforced steel fibrous rectangular concrete beam of cross- section $b \times h$ as follow:

$$M_n = A_s f_y\left(d - \frac{a}{2}\right) + \sigma_t b(h-e)\left(\frac{h}{2} + \frac{e}{2} + \frac{a}{2}\right) \quad (5\text{-}1)$$

$$\sigma_t = 0.00772\frac{\ell}{d_f}\rho_f F_{be} \quad (5\text{-}2)$$

Where σ_t is the tensile stress in fibrous concrete, $\ell$is fiber length, d_f is fiber diameter, ρ_f is the percent by volume of steel fibers, F_{be} is the bond efficiency factor of the fiber which varies from1.0 to 1.2 depending upon fiber characteristics [19], a is the depth of rectangular stress block, d is the distance from extreme compression fiber to centroid of tension reinforcement and e is the distance from extreme compression fiber to top of tensile stress block of fibrous concrete.

Based on the material and geometry described earlier in section 2.0, M_n was calculated for all beam specimens using Eq. (5-1). The stress of main reinforcements was considered yield stress. The tensile stress σ_t is calculated for both PVA and PP fiber in case of specimens which contains the two types of fibers. Therefore, Eq. (5-2) was modified to be:

$$\sigma_t = \sigma_t^{PVA} + \sigma_t^{PP} \quad (5\text{-}3)$$

$\sigma_t^{PVA} = 0.00772\frac{\ell}{d_f}\rho_f F_{be}$ Where = ℓ12 mm, d_f =39 μm and F_{be} =1.0

$\sigma_t^{PP} = 0.00772\frac{\ell}{d_f}\rho_f F_{be}$ Where = ℓ12 mm, d_f =22 μm and F_{be} =1.0

Table 5 shows the comparison between experimental and predicted ultimate moment using ACI 544 equations. It can be concluded good agreements between the experimental and predicted ultimate moment. The average ratio of M_n/M_{exp} for all specimens is 1.07 with 0.12 standard deviation and coefficient of variation equal 10.86%.

6. Conclusions

This investigation studied the flexural performance of specimens containing engineered cementitious composites. Based on the purpose of this investigation and considering the materials used and the comparison of the test and numerical outcomes, the following conclusions can be drawn:

(a) Specimen B1

(b) Specimen B2

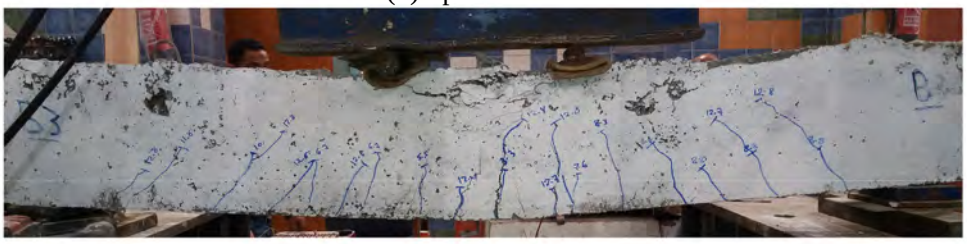

(c) Specimen B3

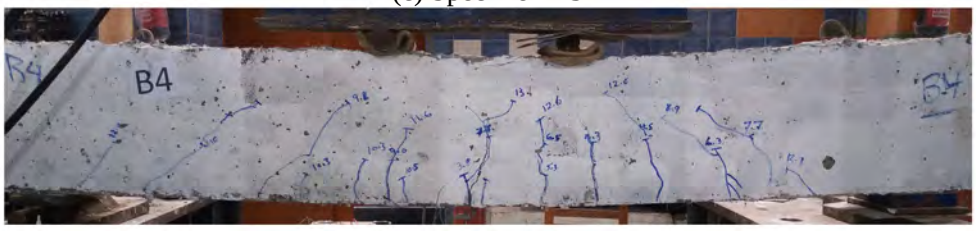

(d) Specimen B4

(e) Specimen B5

(f) Specimen B6

Fig. 7. Cracks pattern of Group A.

(g) Specimen B7

Fig. 7 (*continued*)

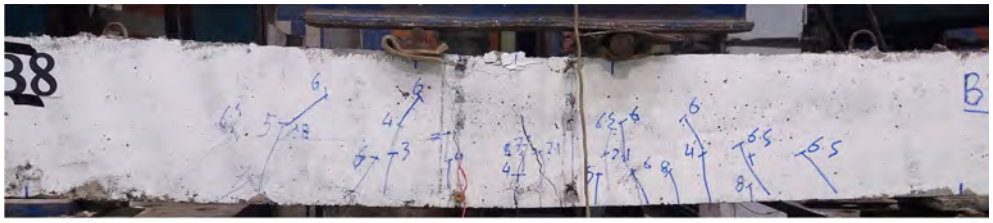

(a) Specimen B8

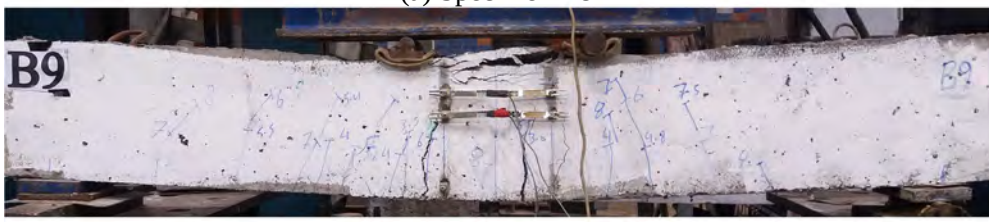

(b) Specimen B9

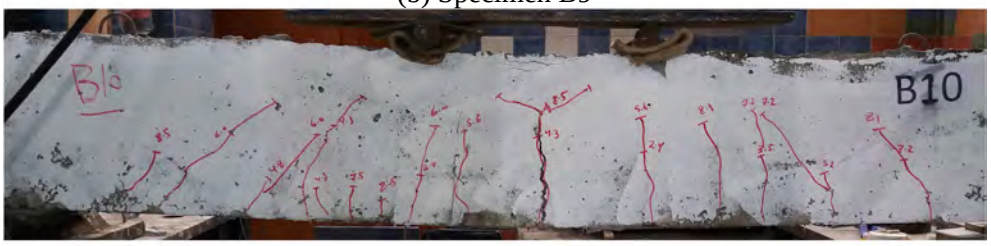

(c) Specimen B10

(d) Specimen B11

(e) Specimen B12

Fig. 8. Cracks pattern of Group B.

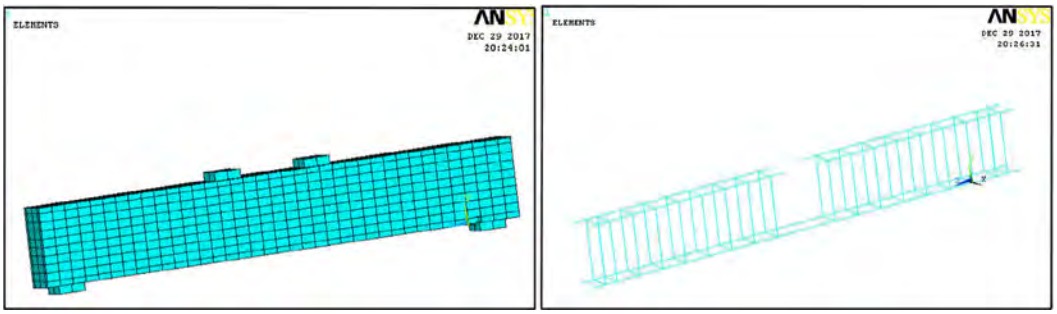

(a) Concrete element; Solid65 (b) Reinforcing bar element; Link8

Fig. 9. Typical idealization of test specimen.

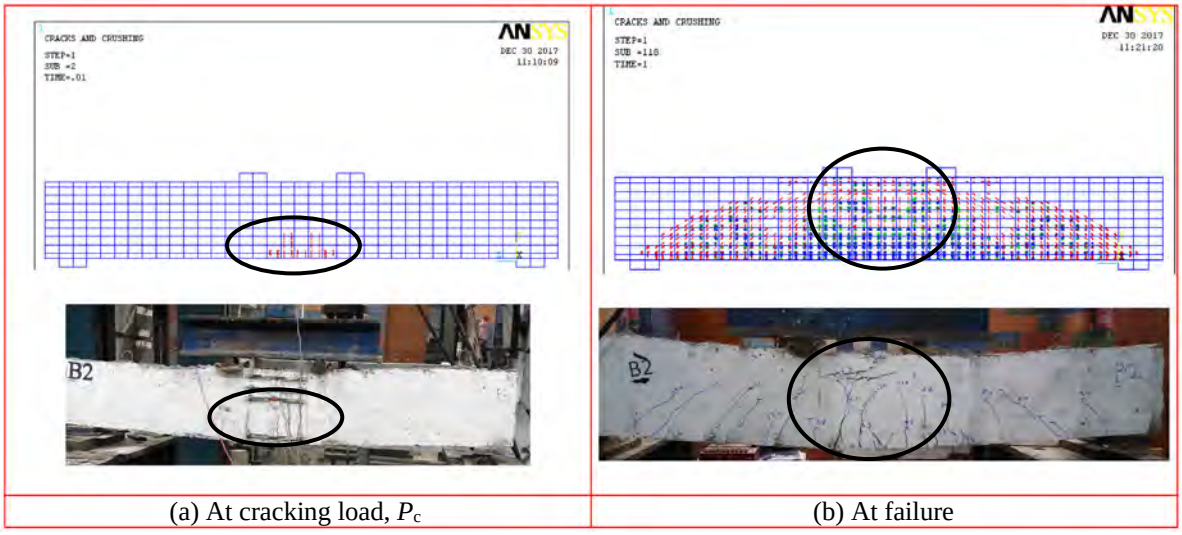

(a) At cracking load, P_c (b) At failure

Fig. 10. Cracks spread for Specimen B2.

Table 4
Comparison of experimental results with NLFEA results.

Specimens	Experimental results		NLFEA results		Numerical results/Experimental results	
	cracking load, $P_{c\text{-exp}}$ (kN)	Failure load, P_{exp} (kN)	cracking load, $P_{c\text{-}nu}$ (kN)	Failure load, P_{nu} (kN)	$(P_{c\text{-nu}})/(P_{c\text{-exp}})$	$(P_{u\text{-nu}})/(P_{u\text{-exp}})$
B1	29.0	115	30	125	1.03	1.09
B2	33.0	138	32	152	0.97	1.10
B3	34.0	154	36	170	1.06	1.10
B4	30.0	127	33	140	1.10	1.10
B5	28.0	143	32	154	1.14	1.08
B6	31.0	144	29	155	0.94	1.08
B7	32.0	139	36	145	1.13	1.04
B8	26.0	81	24	79	0.92	0.98
B9	30.0	89	33	94	1.10	1.06
B10	29.0	101	32	98	1.10	0.97
B11	28.0	96	32	97	1.14	1.01
B12	30.0	109	33	103	1.10	0.94
Mean					1.06	1.05
Standard deviation					0.078	0.057
Coefficient of variation					*7.3%*	*5.4%*

- Generally, ECC fibers in form of PVA exhibits much better behavior than discrete fibers in the form of polypropylene PP. The increase in load carrying capacities when using ECC material can be illustrated by the strain hardening and multiple micro-cracking behavior.
- The maximum load increases as the volume content of fibers increases. The load increases by 20% and 34% for 1.0% and 2.0% of PVA ratio, respectively. The percentage of increase reaches to 11% and 24% when using a mix of both PVA and PP fiber of ratios of 0.5% and 1.0% for B4 and B5, respectively.

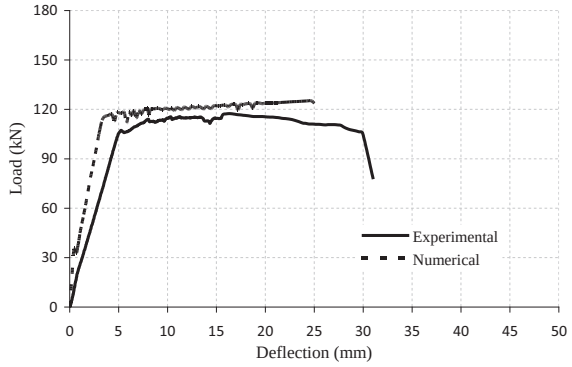

(a) Specimen B1

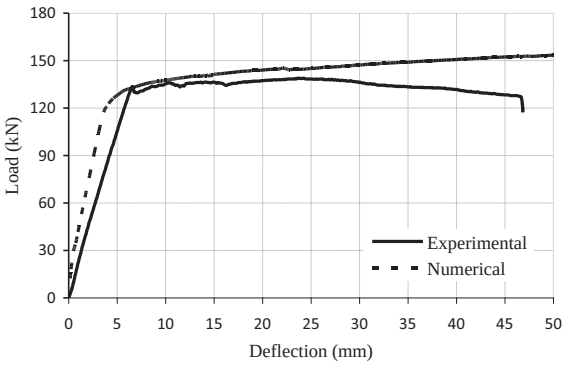

(b) Specimen B2

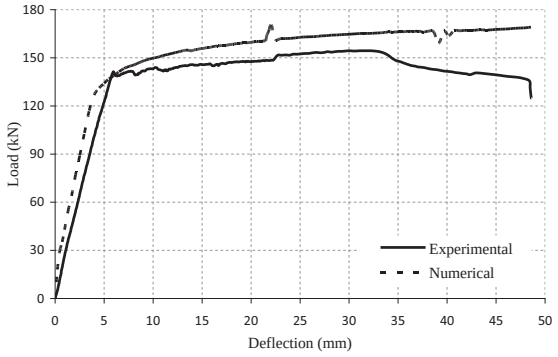

(c) Specimen B3

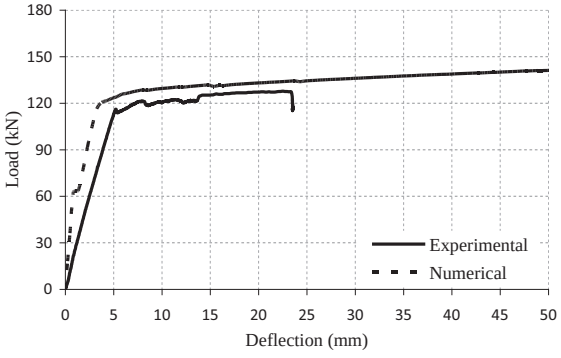

(d) Specimen B4

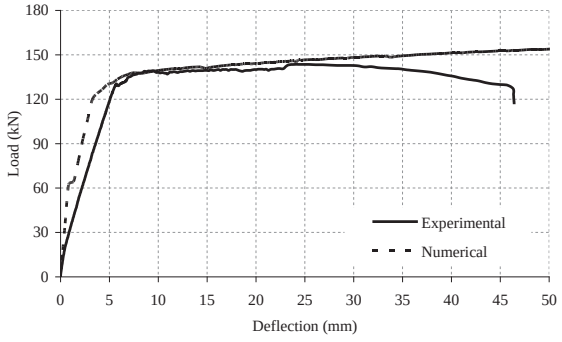

(e) Specimen B5

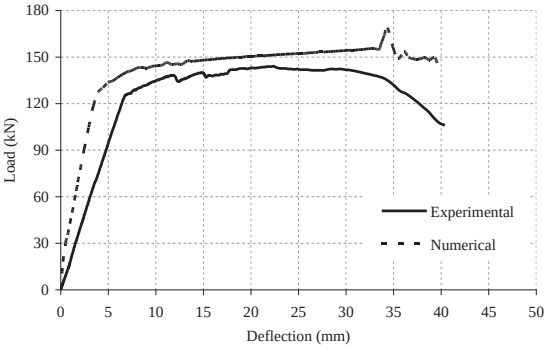

(f) Specimen B6

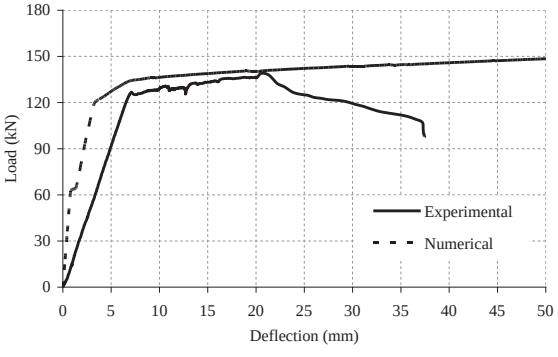

(g) Specimen B7

Fig.11. Comparison of predicted deflections with experimental values of Group A.

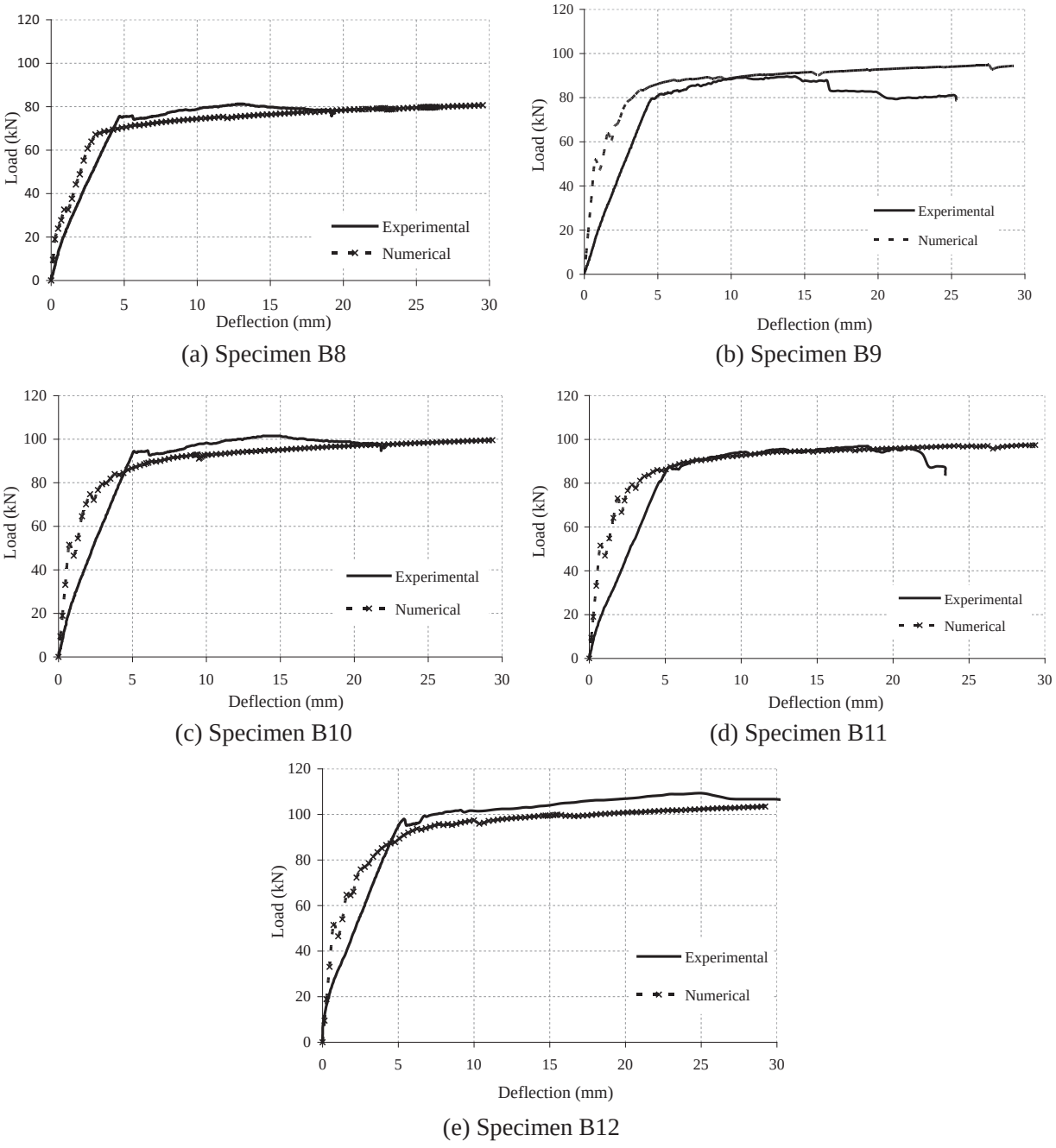

Fig.12. Comparison of predicted deflections with experimental values of Group B.

- A reasonable increasing in the maximum load capacity ranged from 20% to 25% when using a limited layer thickness of PVA concrete (100 mm or 200 mm).
- For lower longitudinal reinforcements ratio, the percentage of increasing in the load reaches to 19% and 39% when using a mixer of both PVA and PP fiber with the ratios of 0.5% and 1.0% for B11 and B12, respectively. It may be revealed that ECC materials improve the behavior more significantly at low reinforcement ratios.
- ECC materials exhibits an improvement in ductility. It reaches its extreme strength in the post- cracking deformation regime. In addition to a relatively large inelastic deformation capability. The relative ductility factor increases, in the total beam section, by 30% and 45% for PVA ratios of 1.0% and 2.0%, respectively.
- Using limited layer thickness of PVA concrete (100 mm thickness layer of the cross section), ductility increases by 32% and 13% for a mix of PVA and PP fiber content ratios of 0.5% and 1.0%, respectively. The optimized usage of PVA material achieved a reasonable ductility, ECC material demonstrates strain hardening property, therefore, the concrete continued to sustained tension load after cracking and the carrying load capacity increased; therefore, most of the recorded failure modes is a compression failure under the loading plated.
- The load-deflection, initial crack load and the maximum load predicted by using nonlinear NLFEA model, using ANSYS software, gave good convention comparing with the experimental results.

Table 5
Comparison of ultimate moment.

Groups	Beam specimen	Fiber content (PVA) V_f %	Fiber content (PP) V_f %	Thickness of Layer (mm)	Experimental failure load, P_{exp} (kN)	Experimental ultimate moment, M_{exp} (kN.m)	ACI 544 Predicted moment M_n (kN.m)	Predicted moment/ Experimental moment M_n/M_{exp}
Group A	B1	0.00	0.00	———	115	37.4	38.00	1.02
	B2	1.00	0.00	280	138	44.9	45.54	1.02
	B3	2.00	0.00	280	154	50.1	52.20	1.04
	B4	0.50	0.50	280	127	41.3	48.21	1.17
	B5	1.00	1.00	280	143	46.5	56.85	1.22
	B6	2.00	0.00	100	144	46.8	46.79	1.00
	B7	1.00	1.00	200	139	45.2	56.35	1.25
Group B	B8	0.00	0.00	———	81	26.3	22.10	0.84
	B9	0.50	0.50	100	89	28.9	29.12	1.01
	B10	1.00	1.00	100	101	32.8	35.68	1.09
	B11	0.50	0.50	200	96	31.2	32.74	1.05
	B12	1.00	1.00	200	109	35.4	42.42	1.20
Mean								1.07
Standard deviation								0.12
Coefficient of variation								10.86%

- The percentage of the predicted to experimental ultimate strength results for the beams was ranged between 0.94 and 1.10, with a mean value of 1.05 and a coefficient of variation, C.O.V, of 5.4%. Implicitly, the analysis revealed the impact of test parameters considered on the load-carrying capacity.
- Comparing the experimental and predicted ultimate moment using ACI 544 equations; good agreements was achieved. The average ratio of M_n/M_{exp} for all specimens is 1.07 with 0.12 standard deviation and coefficient of variation equal 10.86%.

Conflicts of interest

None.

References

[1] ACI Committee 224, "Control of Cracking in Concrete Structures" ACI 224R-01; May 16, 2001; Copyright® 2001, American Concrete Institute.
[2] Alfonso Cobo-Escamilla, Experimental study of flexural behavior of layered steel fiber reinforced concrete beams, J. Civil Eng. Manage. 23 (6) (2017) 806–813, https://doi.org/10.3846/13923730.2017.1319413.
[3] D. Nicolaides, G. Markou, Modelling the flexural behaviour of fibre reinforced concrete beams with FEM, Eng. Struct. 99 (2015) (2015) 653–665.
[4] Doo-Yeol Yoo, Nemkumar Banthia, Young-Soo Yoon, Flexural behavior of ultra-high-performance fiber-reinforced concrete beams reinforced with GFRP and steel rebars, Eng. Struct. 111 (2016) (2016) 246–262.
[5] Fang Yuan, Jinlong Pan, Xu. Zhun, C.K.Y. Leung, A comparison of engineered cementitious composites versus normal concrete in beam-column joints under reversed cyclic loading, Mater. Struct. 2013 (46) (2013) 145–159, https://doi.org/10.1617/s11527-012-9890-6.
[6] M. Kunieda, K. Rokugo, Measurement of crack opening behavior within ECC under bending moment, in: G. Fischer, V.C. Li (Eds.), Proc., Int'l RILEM Workshop HPFRCC in Structural Applications, RILEM SARL, 2006, pp. 313–322.
[7] M. Maalej, V.C. Li, Flexural/tensile strength ratio in engineered cementitious composites, ASCE J. Mater. Civ. Eng. 6 (4) (1994) 513–528.
[8] Min Wua, BjÖrn Johannesson, Mette Geiker, A review: self-healing in cementitious materials and engineered cementitious composite as a self-healing material, Constr. Build. Mater. (2012).
[9] Mohamed Said, Maher A. Adam, Ahmed A. Mahmoud, Ali S. Shanour, Experimental and analytical shear evaluation of concrete beams reinforced with glass fiber reinforced polymers bars, Constr. Build. Mater. 102 (2016) 574–591, https://doi.org/10.1016/j.conbuildmat.2015.10.185.
[10] JinLong Pan, Fang Yuan, Min Luo, KinYing Leung, Effect of composition on flexural behavior of engineered cementitious composites, Sci China Tech Sci 55 (12) (2012) 3425–3433, https://doi.org/10.1007/s11431-012-4990-7.
[11] J.P. Romualdi, J.A. Mandel, Tensile strength of concrete affected by uniformly distributed closely spaced short lengths of wire reinforcement, Proc. ACI J. 61 (6) (1964) 657–671.
[12] N.P. Romualdi, G.B. Batson, Mechanics of crack arrest in concrete, Proc. ASCE Eng. Mech. J. 89 (EM3) (1963) 147–168.
[13] H. Stang, V.C. Li, Classification of fiber reinforced cementitious materials for structural applications, in: M. Prisco, R. Felicetti, G.A. Plizzari (Eds.), Fiber-Reinforced Concretes, Proc, BEFIB 2004, 2004, pp. 197–218.
[14] S.L. Xu, N. Wang, X.F. Zhang, Flexural behavior of plain concrete beams strengthened with ultra high toughness cementitious composites layer, Mater. Struct. 2012 (45) (2012) 851–859, https://doi.org/10.1617/s11527-011-9803-0.
[15] Victor C. Li, Shuxin Wang, Wu Cynthia, Tensile strain-hardening behavior of polyvinyl alcohol engineered cementitious composite (PVA-ECC), ACI Mater. J. (2001) 483–492.
[16] S. Wang, Micromechanics Based Matrix Design for Engineered Cementitious Composites (PhD Thesis), University of Michigan, 2005.
[17] S. Wang, V.C. Li, High early strength engineered cementitious composites, ACI Mater. J. 103 (2) (2006) 97–105.
[18] F. Yuan, J.L. Pan, Y.F. Wu, Numerical study on flexural behaviors of steel reinforced engineered cementitious composite (ECC) and ECC/concrete composite beams, Sci China Tech Sci 57 (2014) 637–645, https://doi.org/10.1007/s11431-014-5478-4.
[19] ACI Committee 544, Design considerations for steel fiber reinforced concrete; (ACI 544.4R-88). Farmington Hills (Michigan, MI): American Concrete Institute; 1988. Re-approved 1999, 1999.
[20] A.N. Dancygier, Z. Savir, Flexural behavior of HSFRC with low reinforcement ratios, Eng. Struct. 28 (2006) (2006) 1503–1512, https://doi.org/10.1016/j.engstruct.2006.02.005.
[21] D. Suji, S.C. Natesan, R. Murugesan, Experimental study on behaviors of polypropylene fibrous concrete beams ISSN 1862-1775 (Online), J. Zhejiang Univ. Sci. A (2007).
[22] ANSYS®, Engineering Analysis System User's Manual, Vol. 1 & 2, and Theoretical Manual; Revision 8.0, Swanson Analysis System Inc., Houston, Pennsylvania, 2004.
[23] Sayed S. Hussein, Assem Abdelalim, Gamal Abdelaziz, Osama Elhariri, Ramy Radwan, Characteristics of Engineered Cementitious Composites Containing Supplementary Cementitious Materials (MSc. Dissertation), Faculty of Engineering, Shoubra, Benha University, Cairo, Egypt, 2015.